Journal of Hydraulic Structures
J. Hydraul. Struct., 2024;10(4):97-114
DOI: 10.22055/jhs.2024.47401.1309

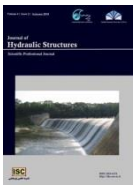

OPEN ACCESS

Optimization of creep function parameters of viscoelastic pipelines based on transient pressure signal

Ebrahim Sharififard [1]
Mohamad Azizipour [*1]
Javad Ahadiyan [2]
Ali Haghighi [1]

Abstract

Determining the creep function of viscoelastic pipes is one of the challenges of modeling these pipes to calibrate or determine defects. The present research aims to determine the creep function of viscoelastic pipes using transient flow pressure in the time and frequency domains. For this purpose, the proposed method is first implemented using a numerical example. The numerical part investigated the effect of signal sample size, the number of Kelvin-Voigt (K-V) elements, repeatability, and decision variables. Then, using an experimental test, the desired methodology has been evaluated. In this research, the K-V mechanical model was used to define the creep function, and its parameters, including elastic pressure wave speed, retardation times, and creep complaint coefficients, were calibrated. The results showed that using pressure signals in both time and frequency domains provides stable results for the investigated pipeline. Examining the effect of signal size showed that the creep function can be estimated with reasonable accuracy in the time domain with a few initial cycles. Also, 14.33 dimensionless frequency for a simple reservoir-pipe-valve system can provide accurate results in the frequency domain. The results of this research can be used as a suitable pre-processing to reduce the dimensions of inputs in models based on artificial intelligence.

Keywords: Creep Function, Polymer Pipe, Water Hammer, Time Domain, Frequency Domain.

Received: 11 July 2024; Accepted: 27 August 2024

[*] Email: azizipour@scu.ac.ir **(Corresponding Author)**
[1] Faculty of Civil Engineering and Architecture, Shahid Chamran University of Ahvaz, Ahvaz, Iran.
[2] Faculty of Water and Environmental Engineering, Shahid Chamran University of Ahvaz, Ahvaz, Iran.

Nomenclature

Symbols and abbreviations

PVC	Polyvinyl chloride	ITA	Inverse transient analysis
PE	Polyethylene	FDS	Frequency domain system
KV	Kelvin-Voigt	TDS	Time domain system
RPV	Reservoir-pipe-valve system	FFT	Fast Fourier transform
MOC	Method of characteristics	GA	Genetic algorithm
ML	Machine learning	HDPE	High-density Polyethylene

1. Introduction

Polymeric pipes such as polyethylene (PE) and polyvinyl chloride (PVC) have many advantages in various applications. First, their good corrosion resistance makes them suitable for transferring fluids with acidic and alkaline properties. These pipes resist extreme temperatures and are highly durable in harsh conditions. In addition, their smooth internal surfaces minimize friction losses. In addition, due to its lightweight and simpler connection compared to other types of pipes, this pipe can have a lower cost of implementation and operation [1, 2].

The unique behavior of polymer pipe walls, which results from their viscoelastic properties, differs considerably from the behavior of elastic pipes. Consequently, the standard water hammer theory is insufficient for accurately describing how viscoelastic pipes respond during transient flow conditions [3, 4]. Unlike elastic metallic pipes, experimental studies have shown that viscoelastic pipelines exhibit greater attenuation and dispersion of transient pressure waves [5- 8]. However, it has also been observed that using viscoelastic pipelines can result in higher maximum transient pressure [9]. Therefore, understanding the response of these pipes during transient flow is crucial for effective design, analysis, and defect detection in such pipeline systems.

Numerous research studies have focused on developing numerical techniques to explain the behavior of viscoelastic pipelines in both the time and frequency domains. When a pressure load is applied to a polymer pipeline, the viscoelastic nature of the material is characterized by an immediate elastic strain followed by a gradual delayed strain. In the time domain, researchers have incorporated a viscoelastic term into the traditional continuity equation and used the method of characteristics to describe the delayed deformation of the pipe walls. The generalized Kelvin-Voigt (K-V) linear viscoelastic mechanical model has been predominantly employed to describe the delayed wall deformation of viscoelastic pipelines [9,10-15]. Various studies have focused on determining the creep function parameters, such as the retardation time scale (τ) and the creep compliance coefficient (j_k), which play a crucial role in representing how strain changes over time under constant stress conditions in the K-V mechanical model [16-19].

Various factors, such as temperature, stress history, and pipe constraints, influence the values of the creep function parameters [16]. Therefore, the parameter values observed during mechanical tests on pipe samples may not match those observed under actual operating conditions. Additionally, the values of these parameters can vary for the same pipe as its length changes [18]. Hence, these parameter values are not unique and can differ [20-22].

To effectively estimate these parameters, transient tests on the specific pipe under investigation are conducted [23-29]. This methodology has been widely used in previous studies to determine the creep function parameters, crucial in representing how strain changes over time under constant stress conditions in the K-V mechanical model. Pezinga [30] obtained the viscoelastic parameters of polymer pipes by calibrating them with a microgenetic algorithm to compare one K-V model and three K-V models. In his research, it was proved that even though

the number of K-V elements is more, the numerical model data are better matched with the experimental data, but still, when it comes to improving the representation of the behavior of polymer materials according to an elastic model., all considered viscoelastic models provide very close results.

According to the literature, the research has not focused on evaluating the different parameters of the pressure signal in the time and frequency domains on the accuracy of creep function estimation. Therefore, the innovation of this research is to evaluate the pressure signal in both time and frequency domains to estimate the creep function.

This research aims to develop a method to determine the parameters of the creep function using the transient pressure signal in the time and frequency domains. For this purpose, different scenarios have been evaluated using a numerical example with a specified creep function. Then, an experimental test was used to assess the research findings.

2. Methodology

2.1. Transient flow governing equations for polymer pipes

In typical engineering applications, equations that describe the 1-D transient flows in the viscoelastic pressurized pipeline are continuity and momentum as follows [1, 31].

$$\frac{\partial H}{\partial t}+\frac{a^2}{gA}\frac{\partial Q}{\partial x}+\frac{2a^2}{g}\frac{d\varepsilon_r}{dt}=0 \tag{1}$$

$$\frac{\partial H}{\partial x}+\frac{1}{gA}\frac{dQ}{dt}+(h_{fs}+h_{fu})=0 \tag{2}$$

where, Q is the discharge, H is the piezometric head, g is the gravity acceleration, A is the area of pipe cross-section, a is the pressure wave speed, $\varepsilon_r$is retarded strain, t is time, x is coordinate along the pipe axis, and h_{fs} and h_{fu} are steady and unsteady friction losses per unit length, respectively.

The steady friction losses are calculated using the Darcy-Weisbach equation. According to a study by [12], unsteady friction can be ignored when the ratio of the radial diffusion timescale to the pressure wave timescale is greater than 1. Based on the characteristics of the pipe system in this research, this ratio is greater than 1, so the parameter of h_{fu} is removed from the momentum equation for more details about the discretization of Eqs. (1) and (2), refer to [23].

2.2. Inverse transient analysis

This section outlines the inverse transient analysis (ITA) approach used to determine the creep function coefficients. The general mathematical model for inverse transient-based determination of creep function parameters for viscoelastic pipes is given by Eq. (3).

$$\{\hat{\boldsymbol{\tau}},\hat{\mathbf{J}},a_e\}=\operatorname{argmin}\left\|\mathbf{h}^{\mathrm{M}}-\mathbf{h}^{\mathrm{S}}(\boldsymbol{\tau},\mathbf{J},a_e)\right\|_2^2 \tag{3}$$

in which $\boldsymbol{\tau}$ and $\mathbf{J}$ are retardation time and creep compliance coefficients vectors in the K-V models, respectively, and the accent mark ⃠ represents the corresponding estimated quantity; a_e is the elastic wave speed and $\mathbf{h}^{\mathrm{M}}$ and $\mathbf{h}^{\mathrm{S}}$ are measured and simulated pressure heads at the same location, respectively.

In Eq. (3), the unknown values are calibrated by minimizing the time or frequency domain signal error. This research used the Genetic algorithm (GA) as an optimization model.

2.3. Numerical model

Due to a lack of details about the creep function parameters in the experimental data, a numerical example was used to analyze the first four subsections. The numerical model simulates a simple pipe system (reservoir-pipe-valve). The pipe has a length of 200 m, an internal diameter of 0.05 m, and a wall thickness of 0.0063 m. The Darcy-Weisbach friction coefficient is 0.02. The speed of the elastic wave is 400 m/s, and the creep function parameters are modeled using three K-V elements with retardation times of $\boldsymbol{\tau} = [0.04, 0.7, 10]$ s and creep compliances coefficient of $\boldsymbol{J} = [0.5, 1.3, 1] \times 10^{-10}$ Pa^{-1}. The upstream reservoir has a pressure head of 40 m, and the steady flow rate is 1.2 L/s.

2.4. Experimental model

The desired laboratory model was built in the Shahid Chamran University of Ahvaz hydraulic laboratory using a simple viscoelastic pipe system. High-density polyethylene pipe (HDPE) (SDR11, PE100, NP16) with nominal diameter (ND) 63 is utilized in this system. Figure 12 shows a schematic and some laboratory photos of the pipeline. In this model, there is a pressure tank with a volume of 600 Liters at the upstream end and two valves at the downstream end to produce transient flow and regulate the flow. The flow rate was measured at the downstream boundary of the pipeline using the volumetric method.

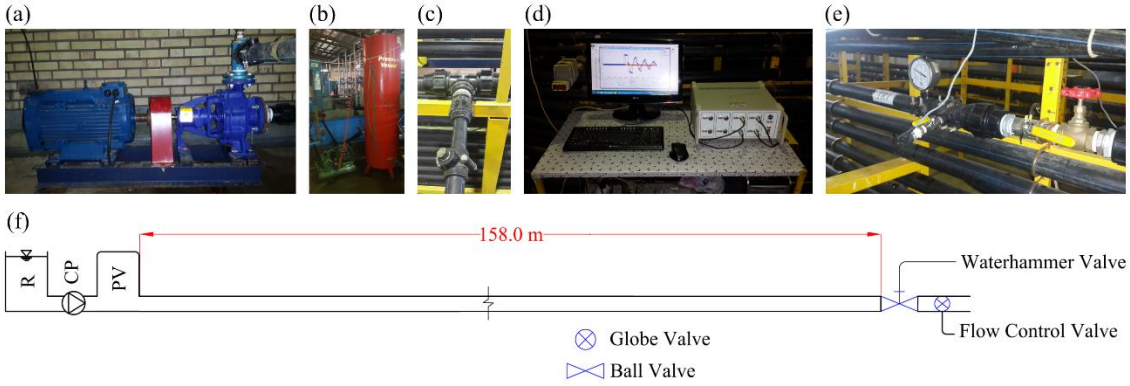

Figure 1. Schematic and some photos of the laboratory system

3. Results and discussion

The results of this section are divided into five subsections. The first part examines the number of K-V elements required for modeling. In the second part, the effect of signal sample size is evaluated in the time and frequency domains. In the third part, the repeatability of the inverse solution method is analyzed. In the fourth section, the effects of retardation time calibration are investigated. The results of the previous four subsections are analyzed in the final section for an experimental test on a polyethylene pipe system.

3.1. Evaluation of the number of K-V element

One of the essential parameters for calibrating the creep function, which is considered based on the K-V model, is the number of elements of this model. In general, it can be said that with the increase in the length of the pipe and its viscous properties, it is necessary to use more elements. In any research for a specific pipe geometry, a preliminary analysis must be done to select the appropriate number of K-V elements. In past research, up to 6 elements have been

included [23]. In this research, four different scenarios have been considered based on the numerical example. At this stage, fixed retardation times have been considered for these four scenarios. As part of the research, a study has also been done on this issue. Therefore, at this stage, only pressure wave speed (a) and creep compliance coefficients (j_k) are considered as unknowns. In the first scenario, the modeling is done based on the elastic pipe, and only the pressure wave speed is calibrated as an unknown by the inverse solution method. A K-V element is considered in the second scenario, and the unknown parameters are two. In the third scenario, two K-V elements are considered for modeling, and there are three unknowns. In the last scenario, the number of K-V elements equals three, and the number of unknowns in the problem is four. It has already been mentioned that these modelings were done based on the pressure signal in the time domain.

Figure 2(a) compares the pressure signal in the time domain for all four scenarios. The results show that, as expected, the elastic model has only been able to model the first half cycle with a relatively good approximation. With the increase of time from the beginning of the transient, the error value of this model has increased. By increasing the viscoelastic model with one element in the second scenario, the accuracy of the modeling has improved significantly compared to the elastic model. The modeling is very close to the actual results in the third scenario with two elements. Finally, in the fourth scenario with three elements, it can be said that the optimal number of K-V elements has been reached, and there is no need to increase the number of model elements. These results are also consistent with the results of [23], and it can be said that three K-V elements are sufficient for the pipe system with this geometry.

In Figure 2 (b), the creep functions of scenarios with 1 to 3 K-V elements are compared with the actual value of the creep function. Also, in Figures 1(c) to 1(e), the values of retardation times, creep compliance coefficients, and elastic pressure wave speed are presented, respectively. According to Figure 1(b), all the creep functions are of the same order. Although the creep functions do not overlap in the complete overview for the model with three K-V elements, according to Figure 3, which shows the first 0.2 s of this comparison, the fourth scenario (with three K-V elements) is the most consistent with this numerical model.

Due to the short length of the pipeline, the initial times are very important, and the creep function has been able to reproduce the pressure signal accurately during these times.

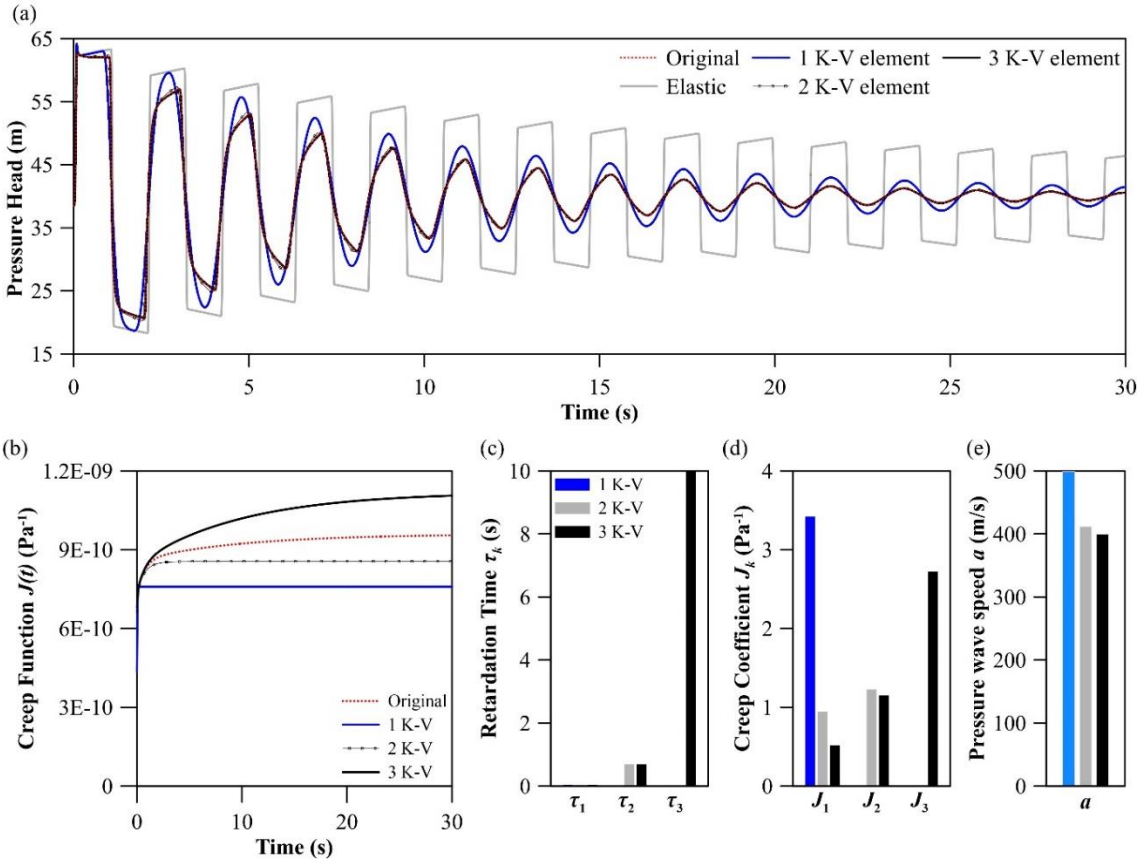

Figure 2. Comparison of (a) pressure signals, (b) creep function, (c) retardation times, (d) creep compliance coefficients, and (e) elastic pressure wave speed of K-V element number determination

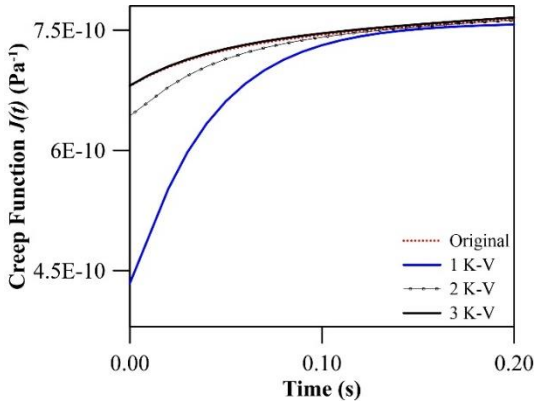

Figure 3. Comparison of creep functions for the initial 0.2 seconds

3.2. Effect of signal sample size on creep function accuracy

This subsection aims to evaluate the effect of signal sample size on the accuracy of creep function estimation. To this end, different signal sizes have been used in the time and frequency domains. In Figure 4, these values are marked in the time and frequency domains using red vertical dashed lines.

A total of six modelings have been done for the time domain signal. Four 5, 10, 20, and 30 s signal sizes have been used for the inverse solution in the first four models. In these models, fixed retardation times are considered. In modeling number 5, in which the modeling time is 30 s, the retardation times are included as 0.05, 0.5, and 5 s. In modeling number 6 with a sample size of 30 s, the retardation times are also calibrated like other parameters.

The results of these six models are presented in Figure 5. Figure 5 (a) compares the calibrated and original pressure signals. Figure 5 (b) shows the calibrated creep functions, and Figure 6 shows the relative error of different models.

The comparison of the modeling sample sizes shows that using the whole signal (30 s) and a few initial cycles (5 s) has been able to accurately estimate the creep function and reproduce the pressure signal. In addition, results from Models 5 and 6 show that Model 5 has more appropriate accuracy. Therefore, it is better to keep the retardation times in a reasonable range (based on previous studies or laboratory mechanical tests) as fixed, and only the creep compliance coefficients and pressure wave speed should be calibrated. Fewer decision variables of model 5 compared to model 6 can increase the efficiency of the optimizer model.

According to [32], because the K-V model is a conceptual model, it cannot be expected that the values of the creep coefficients are the same in different modeling. For example, in the modeling of 30 s and 5 s for the time domain signal, although both models have been able to estimate the creep function with appropriate accuracy, different values for the creep coefficients have been presented in these two modeling combinations. Table 1 shows the details of the optimized parameters of the creep functions.

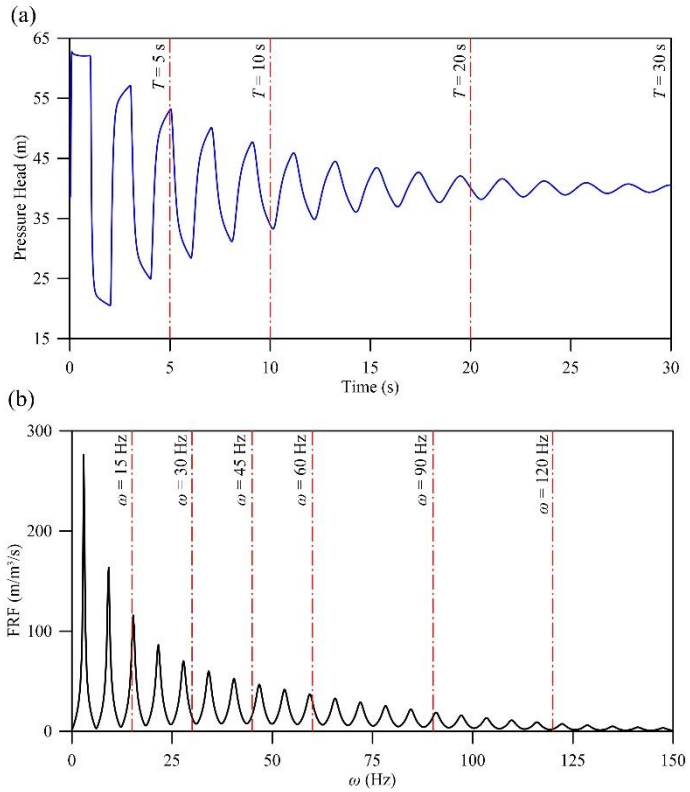

Figure 4. Different sizes of the pressure signal used to determine the creep function in the domain of (a) time and (b) frequency

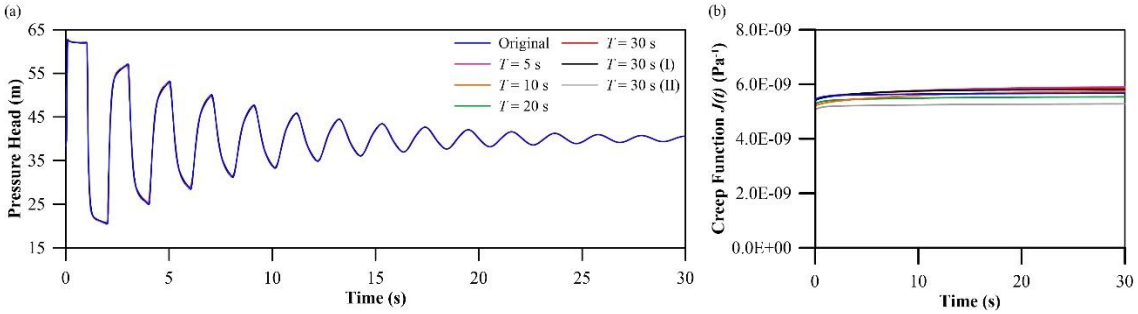

Figure 5. Comparison of (a) pressure wave of different modeling based on different sizes of pressure wave and (b) calibrated creep functions in the time domain

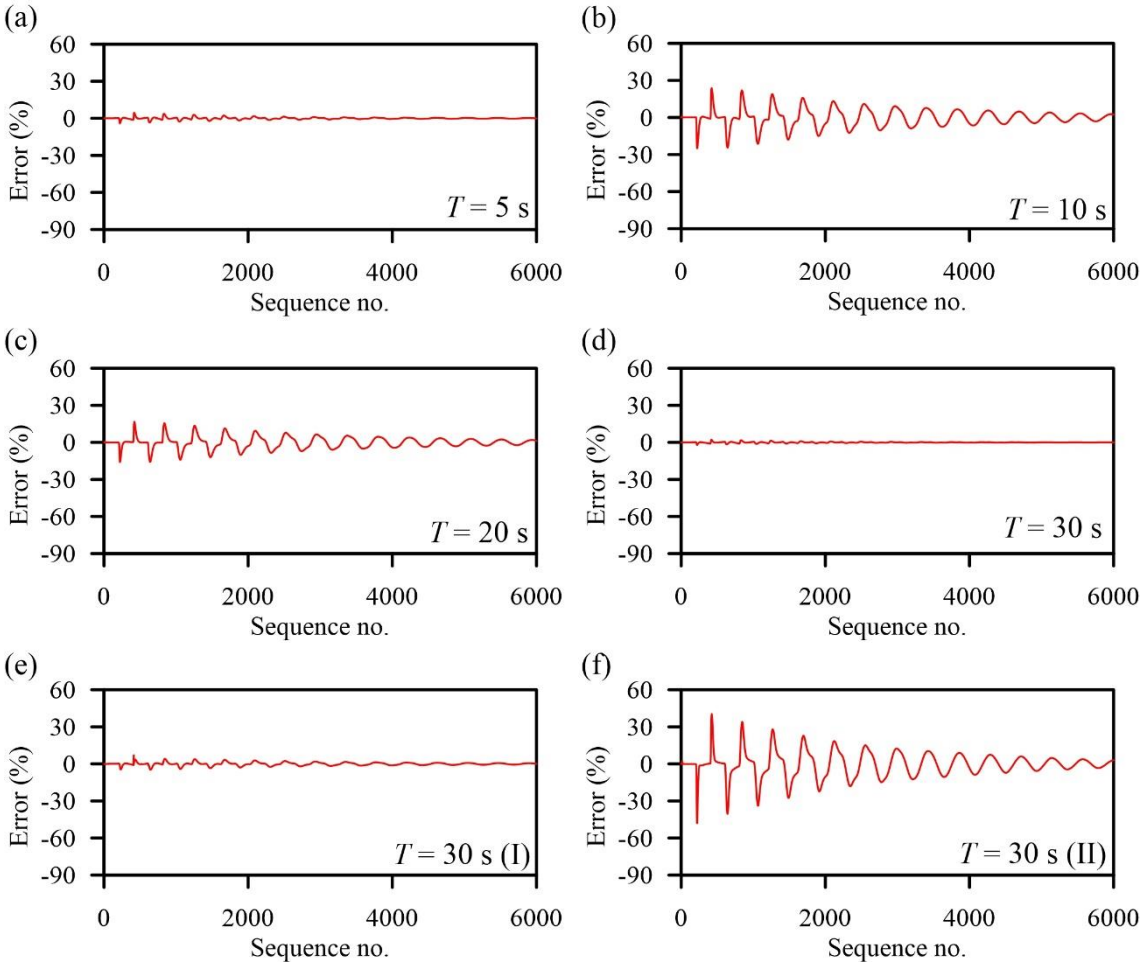

Figure 6 Error between the original and modeled pressure wave for different pressure wave sample sizes in the time domain

Table 1. Details of calibrated creep coefficients based on the size of different signals in the time domain

Test No.	Sample size (s)	τ_1(s)	τ_2(s)	τ_3(s)	$j_1 \times 10^{-10}$	$j_2 \times 10^{-10}$	$j_3 \times 10^{-10}$	a (m/s)
1	5	0.04	0.7	10	0.577	1.010	3.972	401.133
2	10	0.04	0.7	10	0.947	0.827	4.710	409.899
3	20	0.04	0.7	10	0.764	1.166	1.430	406.546
4	30	0.04	0.7	10	0.514	1.150	2.723	399.784
5	30 (I)	0.05	0.5	5	0.599	0.628	3.267	401.619
6	30 (II)	0.014	0.567	13.611	0.961	1.211	1.031	415.366

Six frequency lengths, 15, 30, 45, 60, 90, and 120 Hz, were used to evaluate the estimation of the creep function using the pressure signal in the frequency domain. The results of these six models are presented in Figure 7. Also, the calibrated details of the creep parameters are presented in Table 2. Fixed retardation times are considered in these models. The results of this section showed that the use of low and high-frequency values provides results with lower accuracy, and there is an optimal limit for the frequency sample size used. Based on Figure 8, the 45 and 60 Hz sample sizes have the lowest relative error.

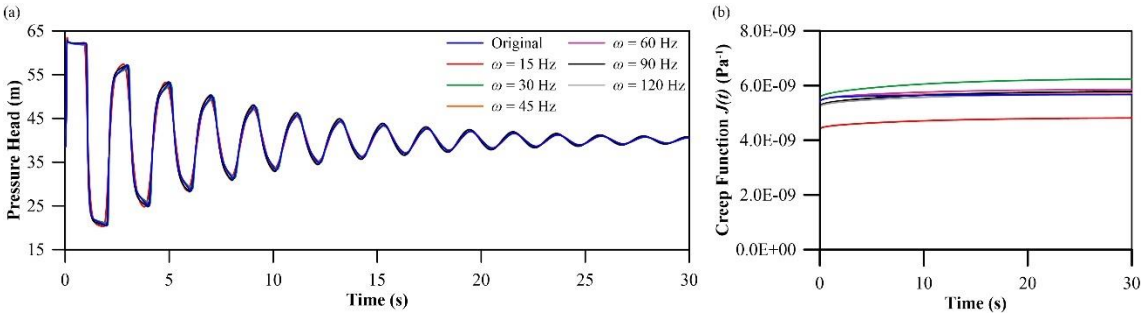

Figure 7. Comparison of (a) pressure signals and (b) creep functions of six different scenarios modeled based on the frequency domain signal

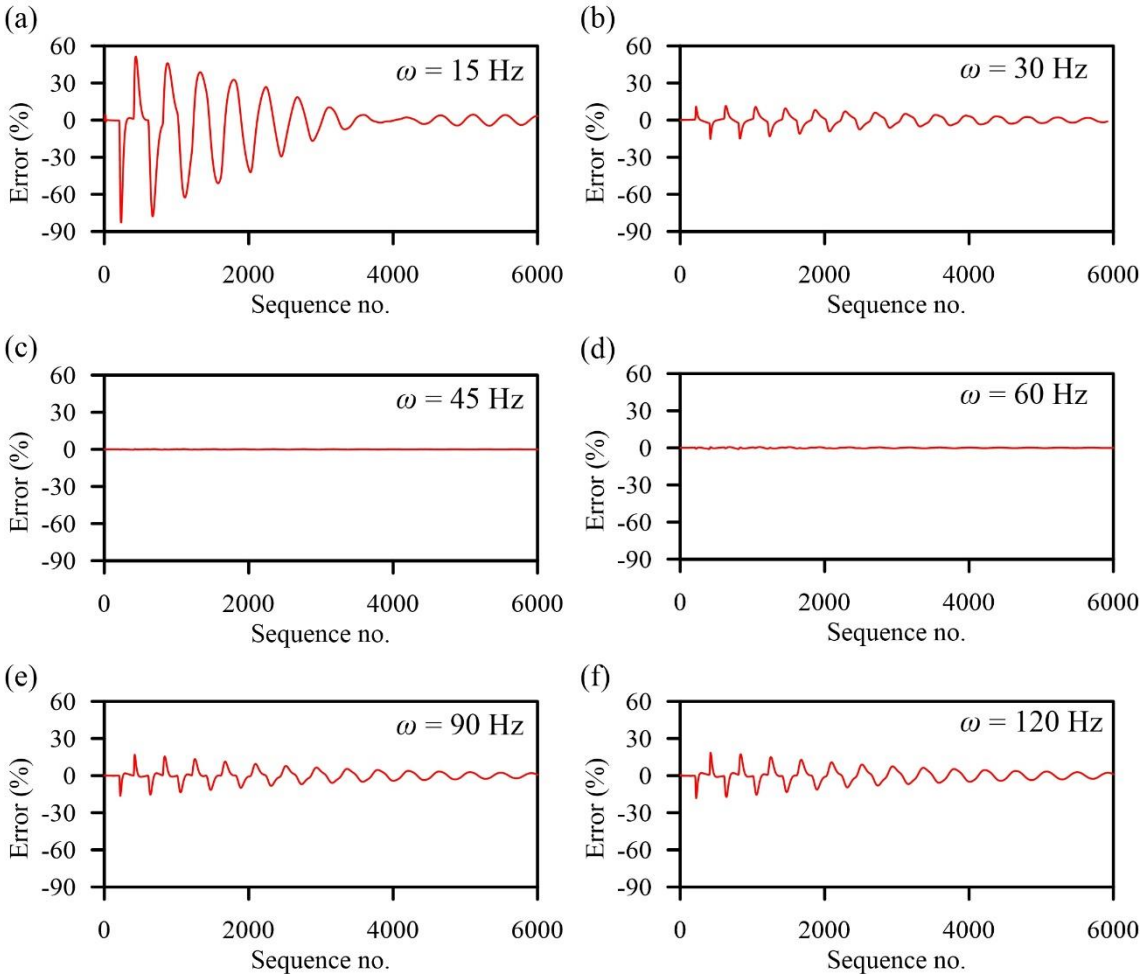

Figure 8. The error between the original and modeled pressure wave for different pressure wave sizes in the frequency domain

Table 2. Details of calibrated creep coefficients based on the size of different signals in the frequency domain

Sample size (ω)	τ_1(s)	τ_2(s)	τ_3(s)	$j_1 \times 10^{-10}$	$j_2 \times 10^{-10}$	$j_3 \times 10^{-10}$	a (m/s)
15	0.04	0.7	10	2.117	0.626	3.269	447.132
30	0.04	0.7	10	0.358	0.920	5.848	394.558
45	0.04	0.7	10	0.507	1.236	1.723	400.006
60	0.04	0.7	10	0.521	1.105	3.197	400.061
90	0.04	0.7	10	0.594	0.818	5.705	401.582
120	0.04	0.7	10	0.71	0.80	4.33	404.21

3.3. Reproducibility of the inverse transient method

One of the important characteristics of a method is its reproducibility with appropriate accuracy. In this sub-section, the reproducibility of the inverse transient method based on pressure signals in both time and frequency domains has been investigated. For this purpose, for a signal with a sample size of 30 s, each model was implemented three times for the pressure signal in the time domain and three times for the pressure signal in the frequency domain. The modeling results for the signal in the time domain are presented in Figure 9, and the modeling results for the pressure signal in the frequency domain are presented in Figure 10.

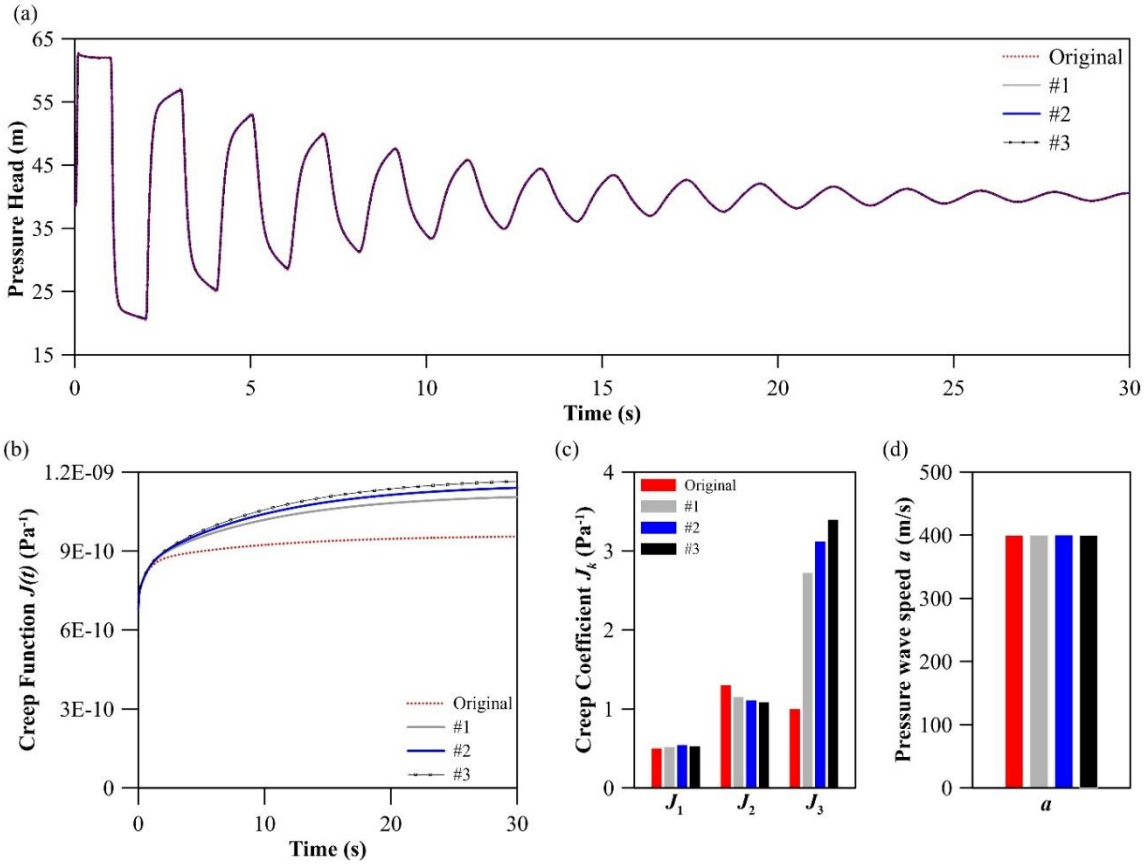

Figure 9 Comparison of (a) pressure signal, (b) creep functions, (c) creep compliance coefficients, and (d) elastic pressure wave speed for three models using the signal in the time domain

According to Figure 9, the model could estimate the creep function and, consequently, the pressure signal accurately in all three runs. Also, according to Figure 10, in the frequency domain, the results of the inverse solution method have been predicted with great accuracy.

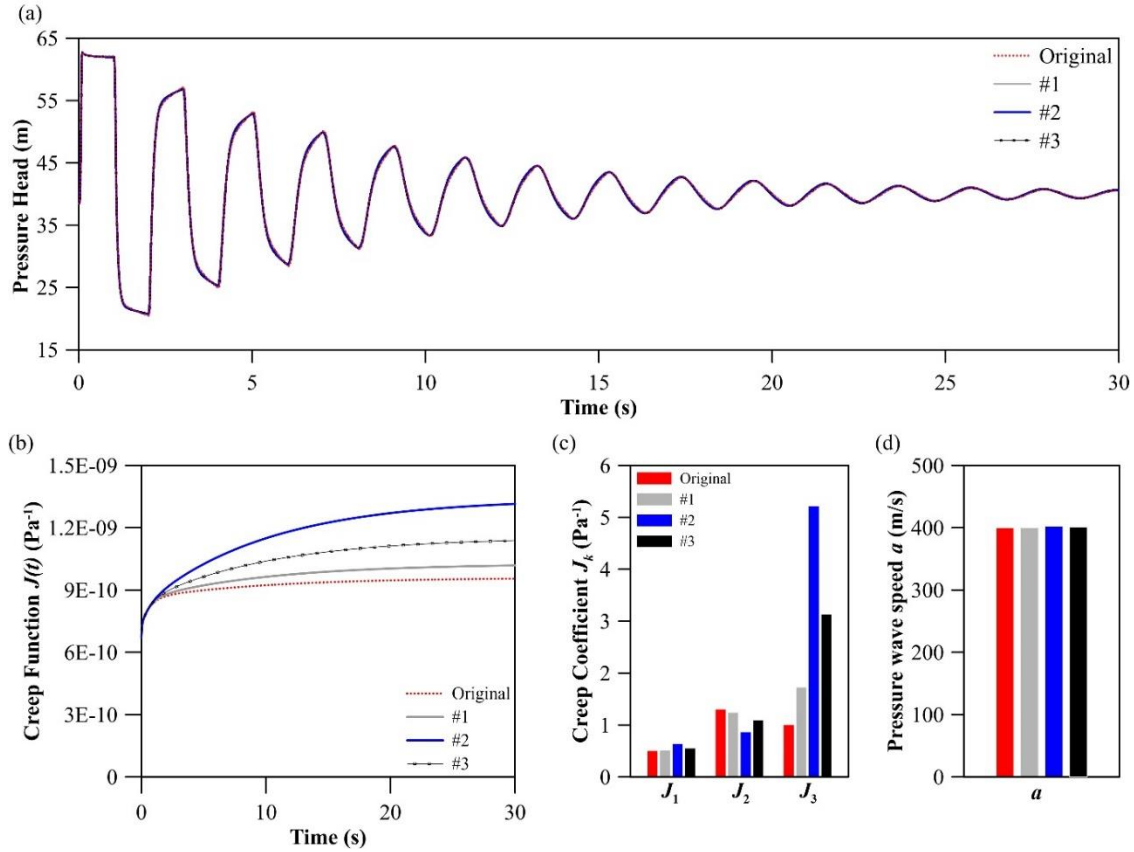

Figure 10. Comparison of (a) pressure signal, (b) creep functions, (c) creep compliance coefficients, and (d) elastic pressure wave speed for three models using signals in the frequency domain

3.4. The effect of retardation times on creep function prediction

One of the unknowns of the creep function in the K-V model is the retardation time (τ). Different approaches regarding these parameters have been used so far. In some research, they are considered constant; in others, these parameters are calibrated. In this subsection, both of these scenarios are implemented. In the first scenario, constant values in the reasonable range provided by [23] are considered; they are regarded as 0.05, 0.5, and 5 s for three elements. Also, in the second scenario, the values of the retardation times are calibrated simultaneously with other parameters of the creep function.

The results of the first scenario based on both pressure signals in the time and frequency domains are presented in Figure 11. The results show that this approach can accurately estimate the creep function. According to the figure, the modelling results based on both types of signals are suitable.

In the second scenario, where all the creep parameters, including elastic pressure wave speed, creep compliance coefficients, and retardation times, are calibrated simultaneously, its results are presented in Figure 12. The results of this scenario are also suitable for both types of signals used. However, considering the benefits of reducing the decision-making variables of the optimizer model, it is better to reduce the decision-making variables to the elastic pressure wave speed and the creep compliance coefficients by choosing appropriate known values for the retardation times.

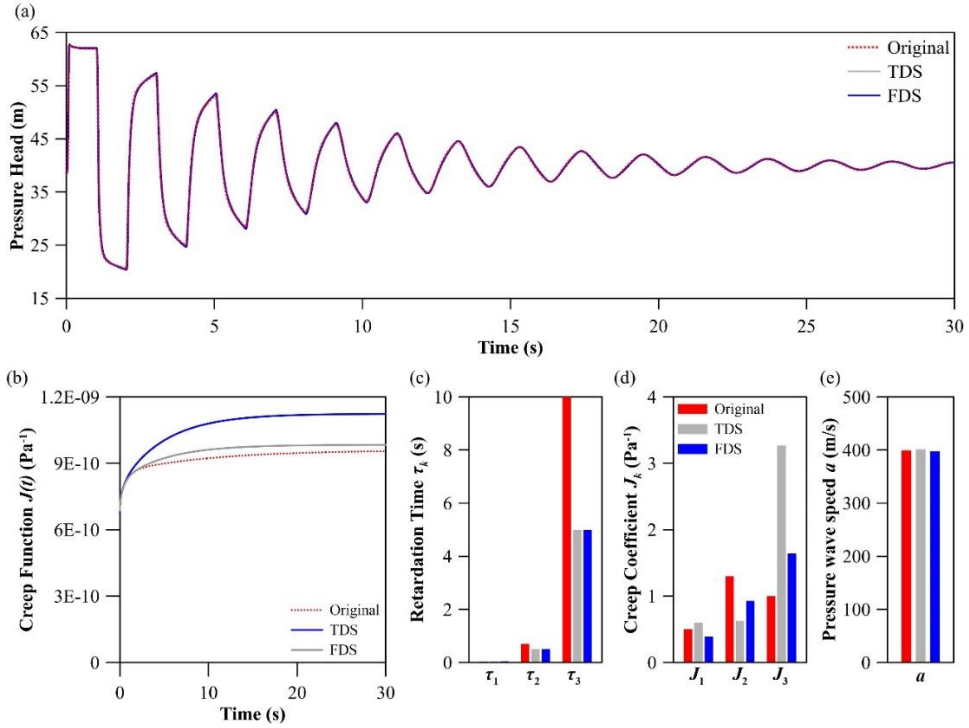

Figure 11. Comparison of (a) pressure signal, (b) creep functions, (c) retardation times, (d) creep compliance coefficients, and (e) elastic pressure wave speed based on known retardation times

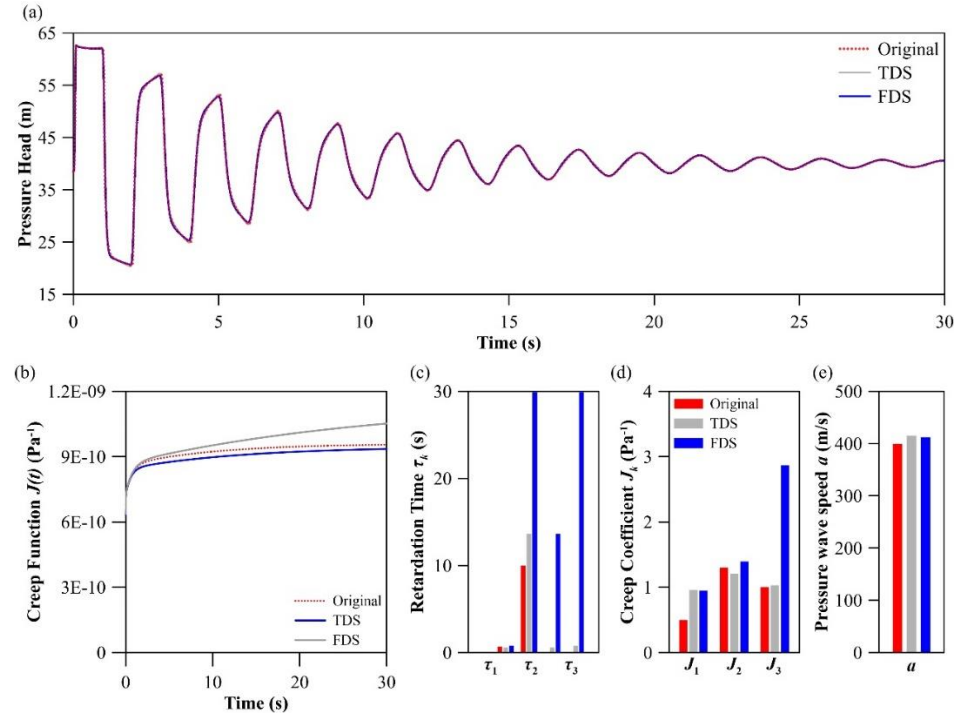

Figure 12 Comparison of (a) pressure signal, (b) creep functions, (c) retardation times, (d) creep compliance coefficients, and (e) elastic pressure wave speed based on calibrated retardation times

3.5. Evaluation based on experimental data

Figure 13 shows the results of time-domain signal-based modeling. Also, the pressure signal in the corresponding frequency domain has been compared with the pressure signal in the time domain. Figure 14 also presents the modeling results based on the frequency domain signal. Figure 15 shows the values of the calibrated creep function. Also, the details of creep function parameters are presented in Table 3. Based on a preliminary analysis, these modelings' values of the retardation times are considered constant as 0.057, 0.4, and 8 seconds, and only the speed of the elastic pressure wave and the creep compliance coefficients for the three Kelvin-Whitt elements has been calibrated. Figure 16 shows the error value of the pressure signal for both methods. The results show that although the pressure signal and the creep function are estimated with appropriate accuracy based on both methods, the modeling accuracy based on the time domain signal is higher.

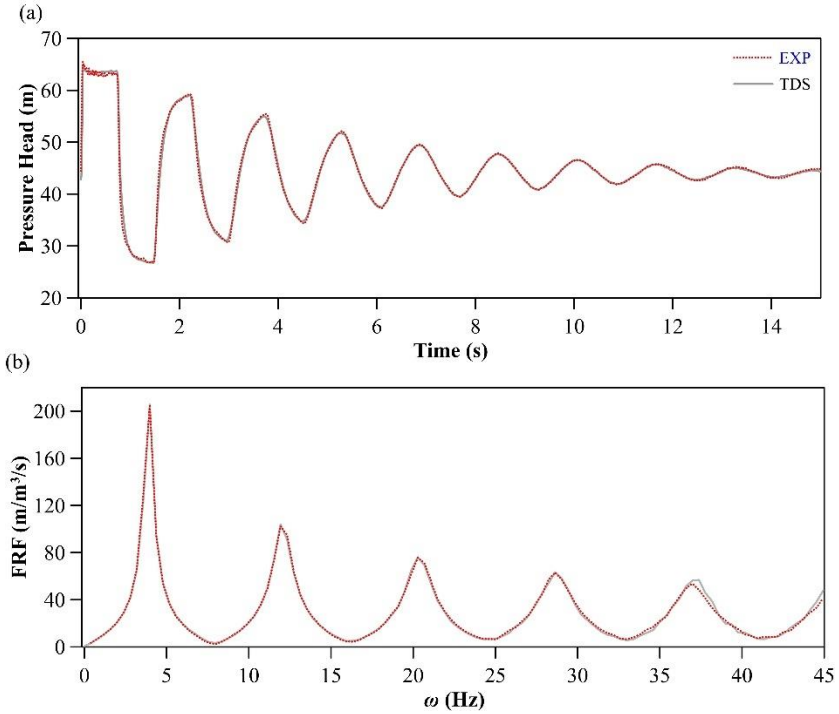

Figure 13. Comparison of pressure signal in (a) time domain and (b) frequency domain for calibrated laboratory sample based on time domain pressure signal

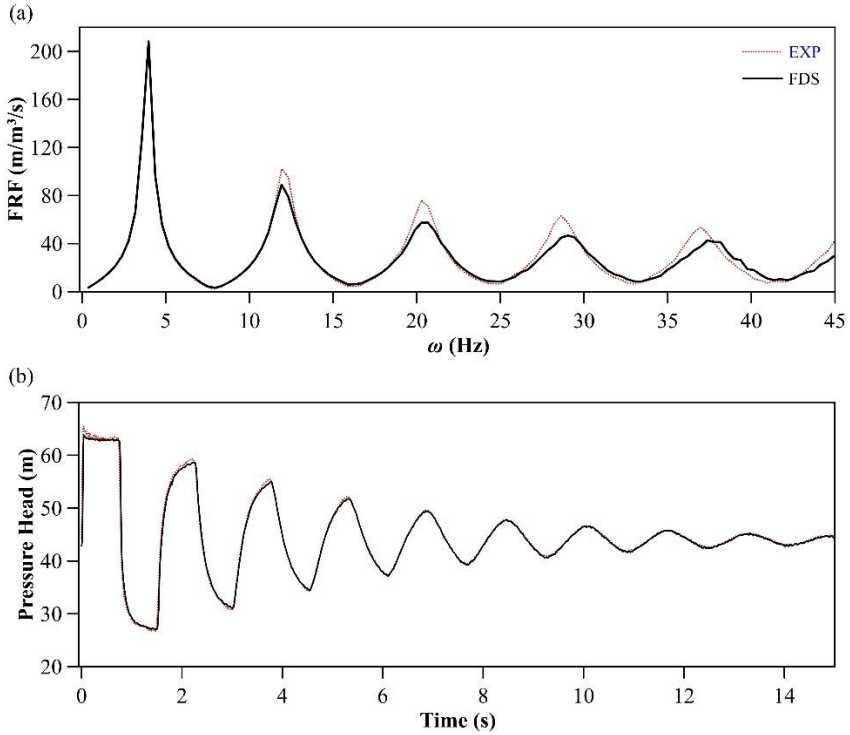

Figure 14. Comparison of the pressure signal in the (a) time and (b) frequency domains for the calibrated laboratory sample based on the frequency domain pressure signal

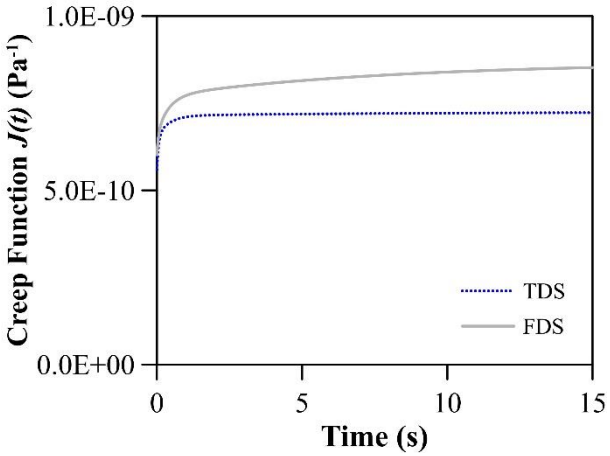

Figure 15. Comparison of the values of the calibrated creep function for the laboratory sample using time and frequency domain signals.

Table 3. Values of the optimized creep parameters for the experimental test

Model	τ_1(s)	τ_2(s)	τ_3(s)	$j_1 \times 10^{-10}$	$j_2 \times 10^{-10}$	$j_3 \times 10^{-10}$	a (m/s)
TDS	0.057	0.4	8	0.930	0.618	0.102	435.44
FDS				0.588	1.085	0.982	421.121

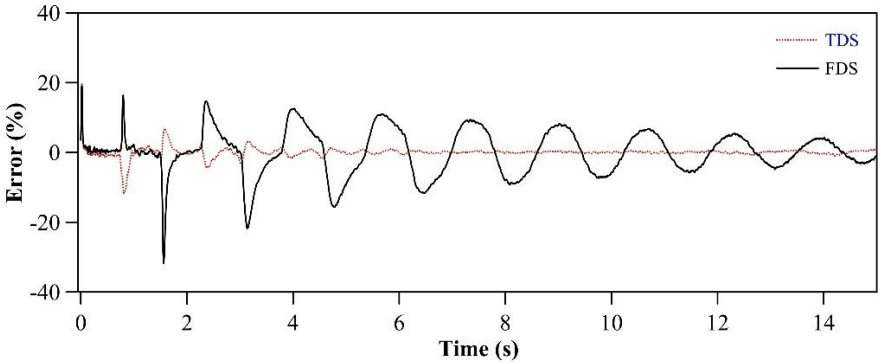

Figure 16 Error between original and calibrated pressure signal and calibrated for both time and frequency domains

4. Conclusion

This research aims to evaluate the creep function estimation of viscoelastic pipes using the inverse transient method based on pressure signals in the time and frequency domain. For this purpose, the effect of various variables, including the number of K-V elements, repeatability, signal sample size, and retardation time optimization, have been investigated. The creep function in this research is considered based on the K-V mechanical element. Also, the genetic algorithm optimization model has been used to determine the decision-making variables. Also, after the preliminary analysis, their results have been validated using an experimental test. The results showed that three K-V elements are sufficient for the pipes on the scale of this research. The effect of the signal size on the accuracy of the creep function estimation showed that with a few initial cycles of the pressure signal in the time domain, the creep function can be determined with reasonable accuracy. Also, the creep function was estimated with appropriate accuracy in the frequency domain with at least the first 40 frequencies of the signal. The evaluation of the effect of optimizing the retardation times showed that the values of these variables can be considered fixed based on similar research or mechanical tests, and their values can be optimized within a reasonable range. The comparison of different models in the time and frequency domain showed that different values for the corresponding creep coefficients were extracted. At the same time, their overall combination provides suitable creep function values. Evaluation of the repeatability of the method used for both signals in the time and frequency domains showed that the model has high stability. The results of this research showed that the estimation of elastic pressure wave speed was estimated with high accuracy in all methods. Results show that both time and frequency domain signals can achieve a reasonable creep function. Although the accuracy of the time domain signal is somewhat higher, the frequency domain signal has a much smaller number of inputs, is suitable for artificial intelligence-based models, and reduces their complexity.

References

1. Keramat, A., Fathi-Moghadam, M., Zanganeh, R., Rahmanshahi, M., Tijsseling, A. S., & Jabbari, E. (2020). Experimental investigation of transients-induced fluid–structure interaction in a pipeline with multiple-axial supports. *Journal of Fluids and Structures*, *93*, 102848.
2. Rahmanshahi, M., Fathi-Moghadam, M., & Haghighi, A. (2018). Leak detection in viscoelastic pipeline using inverse transient analysis. Journal of Water and Wastewater; Ab va Fazilab (in persian), 29(5), 85-97.
3. Williams DJ (1977) Waterhammer in non-rigid pipes: precursor waves and mechanical damping. J Mech Eng Sci 19:237–242.
4. Sharp BB, Theng KC (1987) Water hammer attenuation in uPVC pipe. In: Conference on Hydraulics in Civil Engineering 1987: Preprints of Papers: Preprints of Papers. Institution of Engineers, Australia Barton, ACT, pp 132–136.
5. Brunone B, Berni A (2010) Wall shear stress in transient turbulent pipe flow by local velocity measurement. J Hydraul Eng 136:716–726.
6. Güney MS (1983) Waterhammer in viscoelastic pipes where cross-section parameters are time dependent. In: 4th International Conference on Pressure Surges, England.
7. Meniconi S, Brunone B, Ferrante M, Massari C (2012) Transient hydrodynamics of in-line valves in viscoelastic pressurized pipes: long-period analysis. Exp Fluids 53:265–275.
8. Pezzinga G, Brunone B, Cannizzaro D, et al (2014) Two-dimensional features of viscoelastic models of pipe transients. J Hydraul Eng 140:4014036.
9. Pezzinga G, Scandura P (1995) Unsteady flow in installations with polymeric additional pipe. J Hydraul Eng 121:802–811.
10. Brunone B, Meniconi S, Capponi C (2018) Numerical analysis of the transient pressure damping in a single polymeric pipe with a leak. Urban Water J 15:760–768.
11. Duan H-F, Lee PJ, Ghidaoui MS, Tung Y-K (2012) System response function–based leak detection in viscoelastic pipelines. J Hydraul Eng 138:143–153.
12. Duan H-F, Ghidaoui M, Lee PJ, Tung Y-K (2010a) Unsteady friction and visco-elasticity in pipe fluid transients. J Hydraul Res 48:354–362. https://doi.org/10.1080/00221681003726247.
13. Franke P-G (1983) Computation of unsteady pipe flow with respect to visco-elastic material properties. J Hydraul Res 21:345–353.
14. Keramat A, Tijsseling AS, Hou Q, Ahmadi A (2012) Fluid–structure interaction with pipe-wall viscoelasticity during water hammer. J Fluids Struct 28:434–455.
15. Ramos H, Covas D, Borga A, Loureiro D (2004) Surge damping analysis in pipe systems: modelling and experiments. J Hydraul Res 42:413–425.
16. Covas D, Stoianov I, Ramos H, et al (2004) The dynamic effect of pipe-wall viscoelasticity in hydraulic transients. Part I—experimental analysis and creep characterization. J Hydraul Res 42:517–532. https://doi.org/10.1080/00221686.2004.9641221.
17. Gally M, Gu¨ ney M, Rieutord E (1979) An investigation of pressure transients in viscoelastic pipes.
18. Pezzinga G, Brunone B, Meniconi S (2016) Relevance of pipe period on Kelvin-Voigt viscoelastic parameters: 1D and 2D inverse transient analysis. J Hydraul Eng 142:4016063.
19. Urbanowicz K, Firkowski M, Zarzycki Z (2016) Modelling water hammer in viscoelastic pipelines: short brief. In: Journal of Physics: Conference Series. IOP Publishing, p 12037.
20. Wineman AS, Rajagopal KR (2000) Mechanical response of polymers: an introduction. Cambridge university press.

21. Weinerowska-Bords K (2006) Viscoelastic model of waterhammer in single pipeline-problems and questions. Arch Hydro-Engineering Environ Mech 53:331–351.
22. Weinerowska-Bords K (2007) Accuracy and parameter estimation of elastic and viscoelastic models of water hammer. Task Q 11:383–395.
23. Covas D, Stoianov I, Mano JF, et al (2005) The dynamic effect of pipe-wall viscoelasticity in hydraulic transients. Part II—Model development, calibration and verification. J Hydraul Res 43:56–70.
24. Soares AK, Covas DIC, Reis LFR (2011) Leak detection by inverse transient analysis in an experimental PVC pipe system. J Hydroinformatics 13:153–166. https://doi.org/10.2166/hydro.2010.012.
25. Keramat A, Haghighi A (2014) Straightforward transient-based approach for the creep function determination in viscoelastic pipes. J Hydraul Eng 140:4014058.
26. Weinerowska-Bords K (2015) Alternative approach to convolution term of viscoelasticity in equations of unsteady pipe flow. J Fluids Eng 137.
27. Yao E, Kember G, Hansen D (2016) Water hammer analysis and parameter estimation in polymer pipes with weak strain-rate feedback. J Eng Mech 142:4016052.
28. Yan H, Lam MY, Lee HWJ (2018) Field measurements and theoretical modeling of hydraulic transients in HDPE pipeline with PRV interaction. In: 13th International Conference on Pressure Surges 2018. p 339.
29. Pan B, Duan HF, Meniconi S, et al (2020). Multistage Frequency-Domain Transient-Based Method for the Analysis of Viscoelastic Parameters of Plastic Pipes. J Hydraul Eng 146:1–13.
30. Pezzinga, G. (2023). On the characterization of viscoelastic parameters of polymeric pipes for transient flow analysis. Modelling, 4(2), 283-295.
31. Riyahi, M. M., Rahmanshahi, M., & Ranginkaman, M. H. (2018). Frequency domain analysis of transient flow in pipelines; application of the genetic programming to reduce the linearization errors. Journal of Hydraulic Structures, 4(1), 75-90.
32. Wang X, Lin J, Ghidaoui MS, et al (2020) Estimating viscoelasticity of pipes with unknown leaks. Mech Syst Signal Process 143:106821. https://doi.org/10.1016/j.ymssp.2020.106821.